Strategies in Decision Making in a Multiobjective Context: Integration of DOE, NBI, and CFD in the Optimization of a Centrifugal Fan

Matheus C. Pereira[1], Anderson P. Paiva[1], Matheus B. Francisco[1], Tiago Martins de Azevedo[1]

[1] *Industrial Engineering Institute, Federal University of Itajubá*
BPS Avenue, 1303, Pinheirinho District, ZIP Code: 37550-903, Itajubá, Minas Gerais, Brazil
matheusc_pereira@hotmail.com, andersonppaiva@unifei.edu.br, matheus_brendon@yahoo.com.br, tiago.deazevedo@yahoo.com.br

Abstract. This article evaluates the integration of Design of Experiments, Normal Boundary Intersection, and Computational Fluid Dynamics (CFD) in the fluid dynamic assessment of a centrifugal fan. DOE is used for design preparation, NBI for multiobjective optimization, and CFD for conducting experiments. The obtained results are evaluated using Mahalanobis Distance. The proposed methodology is assessed through a case study involving a centrifugal fan operating under high-speed and high-temperature conditions. The optimizations were confirmed with high reliability, showing an error margin below 15%. This approach aims to contribute to the production of high-performance and resource-efficient fans without extensive simulation and prototyping.

Keywords: Mulitobjective Optimization, Normal Boundary Intersection, Design of Experiments, Centrifugal Fluid Dynamics, Fan.

1 Introduction

Using numerical methods and computational algorithms, Computational Fluid Dynamics (CFD) is employed to solve problems involving fluids and their effects on solid objects. Despite numerous benefits of computationally handling fluids without the need for numerous physical prototypes, there are challenges related to high computational demands [1,2] and the significant time required for complex simulations, leading to long processing times [3,4]. To avoid conducting numerous simulations without a well-defined methodology, Design of Experiments (DOE) is used to guide the appropriate simulations, thereby reducing the number of simulations. With DOE, it is possible to obtain a lot of information with fewer simulations, enabling more robust simulations in less time and with greater reliability.

Once the simulations are performed, the next step is to carry out multiobjective optimization (MO). In this case, the Normal Boundary Intersection (NBI) method is used, which handles MO problems with multiple and often conflicting objectives. To find the appropriate solution, a Pareto Frontier is constructed, showing the set of solutions. This allows verification of the solutions according to the objectives, and NBI has a strong capacity to handle numerous objectives [5]. To evaluate the results obtained from NBI, the Mahalanobis Distance (MD) metric is used, as proposed by Johnson & Wichern [6]. This metric is an "evolution" of the normalized Euclidean distance, with the addition of the variance-covariance matrix.

With the best solution found, a new CFD simulation is conducted using Ansys software to verify if the result obtained with NBI is reliable compared to the CFD simulation. The integration of DOE, CFD, and NBI techniques aims to increase the precision and quality of the results.

The literature addresses the combination of methods such as CFD and MO, as evidenced by various studies, including the performance and emission evaluation of marine combustion engines [7], combustion evaluation in ultra-supercritical boilers [8], thermal management system design for batteries [9], efficiency evaluation of

centrifugal pumps [10], energy performance evaluation of parabolic trough collectors operating with nanofluids [11], aircraft engine turbine evaluation [12], increasing wear resistance in turbines due to erosive particles [13], and the study of airborne infectious disease transmission [14]. The use of NBI for MO with conflicting variables can be seen in Naves et al. [15] Costa et al. [16,17], Lopes et al [18], Belinato et al. [19], Almeida et al [20], Bacci et al. [21].

To demonstrate this approach, a case study of a centrifugal fan is used. This fan operates at high temperatures and speeds within an industrial oven. The material used for the fan is AISI 304. The input variables for this fan are Number of Blades (NB), Initial Angle (IA), Opening Angle (AO), and Blade Length (BL). The experiment conducted was a Central Composite Design (CCD) with 24 experiments where conflicting responses, Mass Flow Rate (MFR) and Torque (T), are evaluated. The goal is to produce a centrifugal fan with the highest MFR and the lowest T, achieving a trade-off between the evaluated responses.

2 Methodology

Initially, it is crucial to define how the simulations will be conducted. A DOE is used to establish the design, and the CCD is recommended. This involves determining the number of input factors, central points, axial points, factorial points, and output variables. With the dependent and independent variables defined, Computer-Aided Design (CAD) is used to design the centrifugal fan. For this activity, Ansys SpaceClaim is utilized. Following this, it is necessary to generate the meshes and perform the CFD simulations, both of which are carried out using Ansys Fluent. The entire process is managed using Ansys Workbench to define and organize the project optimally.

After obtaining the responses from the CFD simulations, the response coefficients are stored for subsequent individual and MO. The individual optimization of the response variables is then performed, which is beneficial for constructing the payoff matrix that contains the utopia and pseudo-nadir values related to the responses found.

A weight scheme is employed to evaluate the responses obtained from the NBI. This results in numerous subproblems, with the number of weight variables corresponding to the number of response variables evaluated. NBI is used to optimize the response variables, generating multiple optimal and viable solutions according to the weights assigned. The general formulation of NBI, adapted from Das and Dennis, can be written as:

$$\begin{cases} \underset{(\mathbf{x},t)}{Max}\, t \\ S.t:\ \overline{\mathbf{\Phi}}\boldsymbol{\beta} + t\hat{\mathbf{n}} = \overline{\mathbf{F}}(\mathbf{x}) \\ \quad \mathbf{x} \in \Omega \\ \quad g_j(x) \le 0 \\ \quad h_j(x) \le 0 \end{cases} \Rightarrow \begin{cases} \underset{(\mathbf{x},t)}{Min}\, -t \\ S.t:\ \overline{\mathbf{F}}(\mathbf{x}) - \overline{\mathbf{\Phi}}\boldsymbol{\beta} - t\hat{\mathbf{n}} = 0 \\ \quad \mathbf{x} \in \Omega \\ \quad g_j(x) \le 0 \\ \quad h_j(x) \le 0 \end{cases} \tag{1}$$

Where: t is a scalar perpendicular to the utopia line, $\overline{\mathbf{\Phi}}$ is the normalized payoff matrix, $\boldsymbol{\beta}$ is the weight vector, $\hat{\mathbf{n}}$ is the quasi-normal vector, and $\overline{\mathbf{F}}(\mathbf{x})$ is the vector of scaled objective functions. Limitations are associated with the optimization algorithm, as gradient-based algorithms are sensitive to the initial starting point.

For each iteration performed, the MD is used to assess the quality of the results obtained. This allows for classifying each response with a metric that indicates how good the solution is compared to others. Additionally, the Pareto Frontier can be plotted to observe the behavior of two output variables, showing how one variable changes with modifications to the other.

Once the optimal results are obtained, Ansys is used again to confirm the optimal result found. This involves repeating the steps of geometry construction, meshing, and simulation to verify the accuracy of the results obtained using the method.

Using this methodology, it is possible to verify the entire process, from experimental planning to validation of the results obtained. This method is promising for product development, allowing for pre-construction verification before prototyping, thereby saving time and resources. Figure 1 illustrates the step-by-step process.

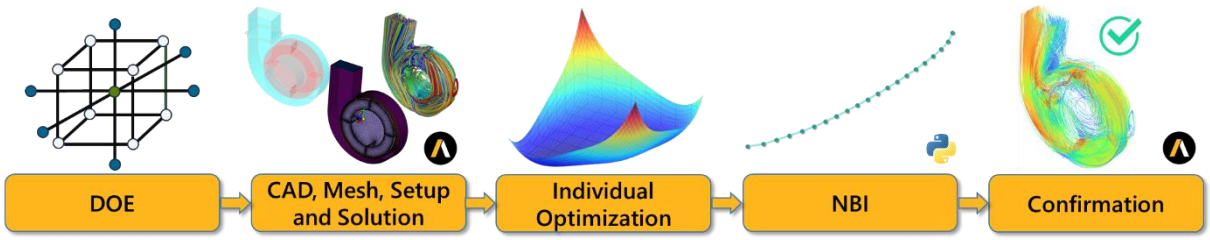

Figure 1. Methodology framework

3 Case Study

To implement the proposed method and verify the benefits and quality of the obtained results, a case study of an industrial centrifugal fan designed for air circulation in an oven is conducted. This fan is made from AISI 304 material, with a density of 7.80 g/m³, specific heat of 0.50 J/kg°C, and thermal conductivity of 16.20 W/m-K. It operates at a rotational speed of 5,500 rpm.

To ensure the quality of the generated meshes, the criteria used are skewness being less than 0.950 and orthogonal quality being greater than 0.150. To verify the convergence of the solutions during the simulation iterations, equations of continuity, velocity in the x, y, and z axes, and turbulence (k and Ω) are considered.

Simulations were performed on 24 different designs, covering the entire process from geometry construction to obtaining results. The dependent variables of the experiment are: Number of Blades (NB), Initial Angle (IA), Opening Angle (OA), and Blade Length (BL). The independent variables are: Mass Flow Rate (MFR), the MFR of the air (study fluid) moving through the fan's cross-section per unit of time, and Torque (T), the amount of rotational force required to turn the fan blades.

The variables MFR and T are highly correlated, with a positive correlation of 0.876 and a covariance of 0.052. The optimization direction for MFR, given in kg/s, is maximization, while for T, given in N·m, it is minimization. The R^2 of the response surface regression model is 0.738 for MFR and 0.801 for T, with standard deviations of 0.043 for MFR and 0.802 for T.

To facilitate understanding, Table 1 presents the results obtained from the DOE simulations, including the coefficients that represent the contribution of each term to the total value of the objective function. Figure 2 shows the dendrogram of clusters using the Ward Linkage Method and Euclidean distance measure, illustrating how the experiments cluster into five groups. Contour plots are provided, showing the velocity magnitude of the fan as represented by a central plane, with all experiments depicted on the same scale.

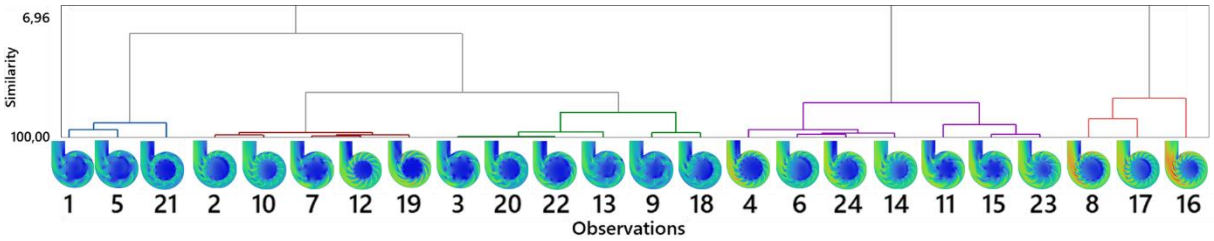

Figure 2. Cluster Dendrogram of Experiments

Table 1. Input and response variables and coefficients

NB	IA	OA	BL	MFR	T	COEF(MFR)	COEF (T)
6	0.00	0.00	26.00	0.214	1.499	0.270	3.358
14	0.00	0.00	26.00	0.266	2.353	0.026	0.602
6	30.00	0.00	26.00	0.219	2.155	-0.005	0.402
14	30.00	0.00	26.00	0.258	3.509	0.012	0.266
6	0.00	90.00	26.00	0.223	1.681	0.011	0.161
14	0.00	90.00	26.00	0.313	3.308	0.016	0.145
6	30.00	90.00	26.00	0.232	2.412	-0.009	-0.237
14	30.00	90.00	26.00	0.339	5.180	-0.013	-0.355
6	0.00	0.00	40.00	0.245	1.850	-0.004	-0.128
14	0.00	0.00	40.00	0.279	2.408	0.000	0.129
6	30.00	0.00	40.00	0.246	2.873	0.018	0.370
14	30.00	0.00	40.00	0.213	2.389	-0.007	-0.170
6	0.00	90.00	40.00	0.263	2.249	0.011	0.192
14	0.00	90.00	40.00	0.320	3.416	-0.002	-0.008
6	30.00	90.00	40.00	0.263	3.158	0.006	0.127
14	30.00	90.00	40.00	0.387	5.793		
18	15.00	45.00	33.00	0.354	4.715		
10	-15.00	45.00	33.00	0.255	1.961		
10	45.00	45.00	33.00	0.181	2.428		
10	15.00	-45.00	33.00	0.226	2.169		
10	15.00	135.00	33.00	0.176	1.279		
10	15.00	45.00	19.00	0.210	2.175		
10	15.00	45.00	47.00	0.270	3.092		
10	15.00	45.00	33.00	0.270	3.358		

4 Results

4.1 Individual Optimization

To understand how the variables behave when another is optimized, a Payoff Matrix is constructed, as shown in Table 2. The main diagonal displays the utopia values for each response variable, while the secondary diagonal shows the pseudo-nadir values. For conflicting variables, such as MFR and T, as one variable approaches its optimum, the other will consequently move away from its optimum. This helps facilitate the MO stage. It is important to note that the algorithm used for the optimizations was the Generalized Reduced Gradient (GRG).

Table 2. Payoff matrix

	MFR	T
MFR	0.400	0.194
T	5.509	1.061

4.2 Normal Boundary Intersection

To generate optimal Pareto solutions and evaluate results in scenarios with conflicting variables, the NBI method is used. This method allows decision-makers to have a grid of options with a low computational cost, especially compared to exhaustive CFD simulations, and aids in understanding the optimal solutions obtained.

A weight increment (w) of 5% was assigned in this process, with each weight associated with a response.

The grid of points was generated using a DOE Simplex-Lattice, where two weights are combined for each objective. This results in 21 optimal and viable solutions. To verify the quality of these optimal solutions, the MD is used to determine the distance between a point and the set of points found, taking into account the correlation and covariance between variables. MD surpasses the Normalized Euclidean Distance (NED) because the best results given by NED tend to zero out some of the weights, turning the problem from multiobjective to single-objective, which is not the evaluation's purpose.

In gradient-based algorithms, the initial point influences the outcomes. Therefore, after individual optimization, an average of the controllable variables was calculated and set as the initial point for each NBI iteration.

Pareto Frontier represents the set of optimal and viable solutions in the context of objective optimization, showing that one objective cannot be improved without worsening another. The results obtained with NBI are illustrated in Figure 3, which shows the generated Pareto Frontier.

Using the MD metric to evaluate the best results, Table 3 displays the input configurations that should be used to obtain the top three MD metrics. The goal is to optimize both variables by minimizing the distance to the utopia point.

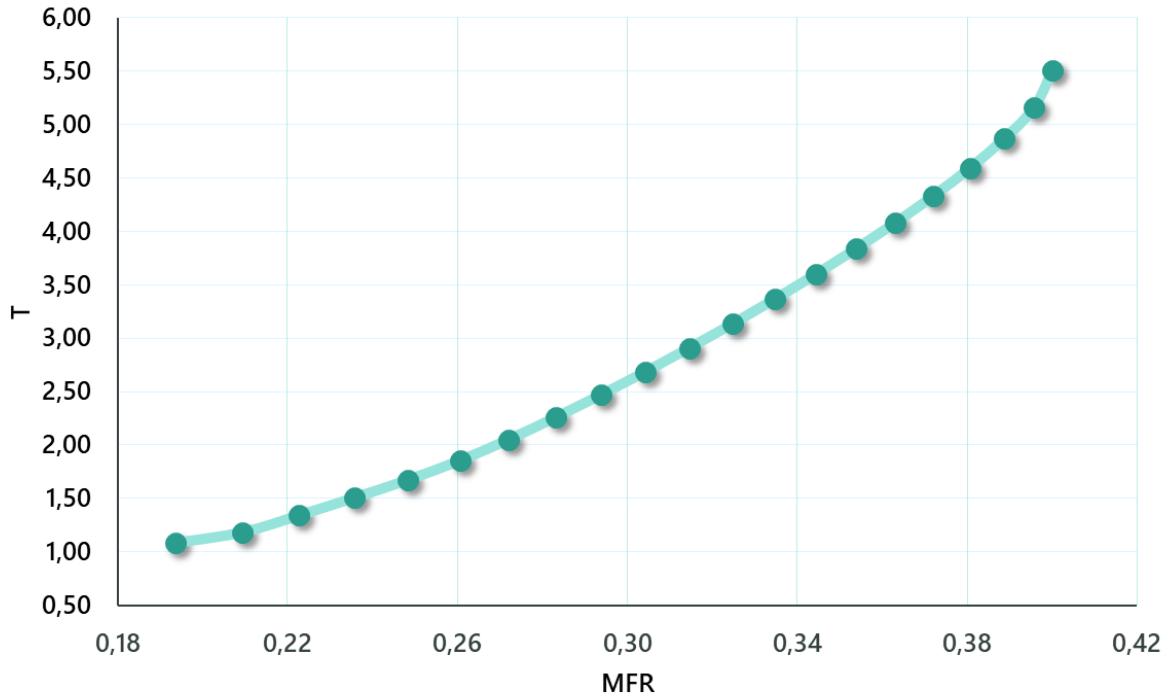

Figure 3. Pareto front of mass flow rate and torque responses

Table 3. Best results with Mahalanobis distance

w_1	w_2	NB	IA	OA	BL	MD
0.350	0.650	4	-3.70	28.85	35.87	0.625
0.300	0.700	6	-7.65	25.42	37.44	0.710
0.750	0.250	17	0.28	56.21	34.93	0.930

It is observed that the two smallest MD values prioritize the weight w_2, which corresponds to T, while the third smallest MD result prioritizes the weight w_1, corresponding to the MFR. Thus, it is noted that the solution favoring MFR has a higher NB and an IA, while the other variables do not significantly change relative to the responses obtained.

By evaluating the standardized effects and performing an analysis of variance (ANOVA), the importance of the variables is determined. Considering p-values less than 0.050, MFR shows greater importance for MFR (p-

value of 0.036), while T shows greater importance for NB (p-value of 0.013) and IA (p-value of 0.037).

4.3 Results of Computational Fluid Dynamics

After completing the optimization process and determining which solution to replicate, the results are validated using Ansys software. A comparison is made between the optimization results and those obtained from the simulation. Figure 4 illustrates the geometry, meshes, and contour lines related to particle movement. The closer the value is to red, the higher it is, while the closer it is to blue, the lower it is.

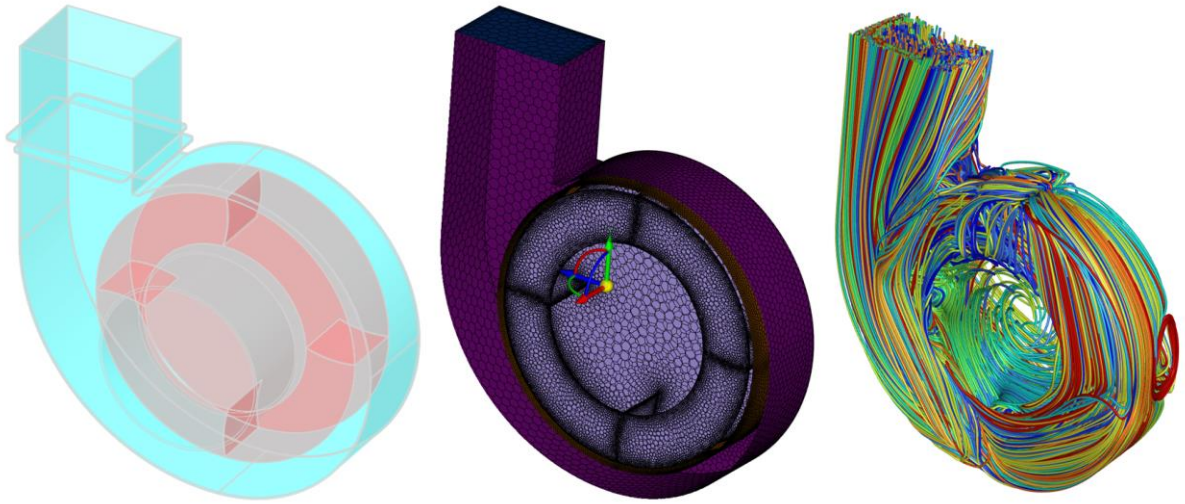

Figure 4. Geometry, mesh, and pathlines of the ideal centrifugal fan

The results for MFR and T after 1,000 iterations and achieving the defined convergence criteria are as follows: the MFR result was 0.238 kg/s, while the T was 2.214 N·m. Both results were very similar to those provided by the NBI method, achieving an accuracy of over 85.00% for both responses.

The variables have opposing optimization directions and natural dependencies, meaning that improving one may worsen the other. Therefore, it is crucial to clearly define the design and performance objectives of the product to assist in the decision-making process, which can impact the optimization process.

The replicated fan has 4 blades, an initial angle of -3.70º, an opening angle of 28.85º, and a blade length of 35.87 mm. The blade thickness and width are fixed variables with respective values of 0.80 mm and 44.60 mm.

5 Conclusions

This article aims to combine DOE techniques to plan and conduct experiments, and NBI for MO, utilizing CFD for fluid dynamics simulations. This approach is used to simulate the experiments generated by the design and to confirm the optimal and viable result with the lowest MD value.

By employing and integrating these techniques, it becomes possible to identify the best parameters, determine the factors that have the most influence on the responses, and simultaneously optimize the criteria. This creates a robust method for achieving these objectives, and the proposed approach is applied in a case study involving a centrifugal fan to verify the precision of the method.

In the case study, the proposed method performed well, as the results obtained from validation were accurate and showed better-than-expected performance. This validation can lead to improved fan performance without the need for numerous simulations or physical prototypes, thus saving resources and time.

For future work, the initialization of the algorithm will be carried out with multiple starting points to understand how this influences the algorithm's performance. Additionally, optimization will be performed using the Non-dominated Sorting Genetic Algorithm II (NSGA-II) for comparison with the NBI.

Acknowledgements. Thanks are expressed to CAPES, CNPq, and FAPEMIG for the support provided to this work. This research was also made possible by the support of NOMATI-UNIFEI, which provided access to their laboratories, materials, and expertise.

Authorship statement. The authors hereby confirm that they are the sole liable persons responsible for the authorship of this work, and that all material that has been herein included as part of the present paper is either the property (and authorship) of the authors, or has the permission of the owners to be included here.

References

[1] Raman V, Hassanaly M. Emerging trends in numerical simulations of combustion systems. *Proc Combust Inst* 2019;37:2073–89. https://doi.org/10.1016/j.proci.2018.07.121.
[2] Li G, Wang H, Zhang M, Tupin S, Qiao A, Liu Y, et al. Prediction of 3D Cardiovascular hemodynamics before and after coronary artery bypass surgery via deep learning. *Commun Biol* 2021;4:99. https://doi.org/10.1038/s42003-020-01638-1.
[3] Liu Y, Lu Y, Wang Y, Sun D, Deng L, Wang F, et al. A CNN-based shock detection method in flow visualization. *Comput Fluids* 2019;184:1–9. https://doi.org/10.1016/j.compfluid.2019.03.022.
[4] Casas CQ, Arcucci R, Wu P, Pain C, Guo YK. A Reduced Order Deep Data Assimilation model. *Phys D Nonlinear Phenom* 2020;412:132615. https://doi.org/10.1016/j.physd.2020.132615.
[5] Das I, Dennis JE. Normal-Boundary Intersection: A New Method for Generating the Pareto Surface in Nonlinear Multicriteria Optimization Problems. *SIAM J Optim* 1998;8:631–57. https://doi.org/10.1137/S1052623496307510.
[6] Johnson RA, Wichern DW. Applied multivariate statistical analysis. 1982.
[7] Tan D, Wu Y, Lv J, Li J, Ou X, Meng Y, et al. Performance optimization of a diesel engine fueled with hydrogen/biodiesel with water addition based on the response surface methodology. *Energy* 2023;263:125869. https://doi.org/10.1016/j.energy.2022.125869.
[8] Shi Y, Zhong W, Chen X, Yu AB, Li J. Combustion optimization of ultra supercritical boiler based on artificial intelligence. *Energy* 2019;170:804–17. https://doi.org/10.1016/j.energy.2018.12.172.
[9] Li W, Peng X, Xiao M, Garg A, Gao L. Multiobjective design optimization for mini-channel cooling battery thermal management system in an electric vehicle. *Int J Energy Res* 2019;43:3668–80. https://doi.org/10.1002/er.4518.
[10] Wang C-N, Yang F-C, Nguyen VTT, Vo NTM. CFD Analysis and Optimum Design for a Centrifugal Pump Using an Effectively Artificial Intelligent Algorithm. *Micromachines* 2022;13:1208. https://doi.org/10.3390/mi13081208.
[11] Abubakr M, Amein H, Akoush BM, El-Bakry MM, Hassan MA. An intuitive framework for optimizing energetic and exergetic performances of parabolic trough solar collectors operating with nanofluids. *Renew Energy* 2020;157:130–49. https://doi.org/10.1016/j.renene.2020.04.160.
[12] Wang Y, Liu T, Zhang D, Xie Y. Dual-convolutional neural network based aerodynamic prediction and multiobjective optimization of a compact turbine rotor. Aerosp Sci Technol 2021;116:106869. https://doi.org/10.1016/j.ast.2021.106869.
[13] Aponte RD, Teran LA, Grande JF, Coronado JJ, Ladino JA, Larrahondo FJ, et al. Minimizing erosive wear through a CFD multiobjective optimization methodology for different operating points of a Francis turbine. *Renew Energy* 2020;145:2217–32. https://doi.org/10.1016/j.renene.2019.07.116.
[14] Arjmandi H, Amini R, khani F, Fallahpour M. Minimizing the respiratory pathogen transmission: Numerical study and multiobjective optimization of ventilation systems in a classroom. *Therm Sci Eng Prog* 2022;28:101052. https://doi.org/10.1016/j.tsep.2021.101052.
[15] Naves FL, Paula TI de, Balestrassi PP, Braga WLM, Sawhney RS, Paiva AP de. Multivariate Normal Boundary Intersection based on rotated factor scores: A multiobjective optimization method for methyl orange treatment. *J Clean Prod* 2017;143:413–39. https://doi.org/10.1016/j.jclepro.2016.12.092.
[16] Costa DMC, Brito TG, Paiva AP de, Leme RC, Balestrassi PP. A normal boundary intersection with multivariate mean square error approach for dry end milling process optimization of the AISI 1045 steel. *J Clean Prod* 2016;135:1658–72. https://doi.org/10.1016/j.jclepro.2016.01.062.
[17] Costa DMD, Paula TI, Silva PAP, Paiva AP. Normal boundary intersection method based on principal components and Taguchi's signal-to-noise ratio applied to the multiobjective optimization of 12L14 free machining steel turning process. *Int J Adv Manuf Technol* 2016;87:825–34. https://doi.org/10.1007/s00170-016-8478-7.
[18] Lopes LGD, Brito TG, Paiva AP, Peruchi RS, Balestrassi PP. Robust parameter optimization based on multivariate normal boundary intersection. *Comput Ind Eng* 2016;93:55–66. https://doi.org/10.1016/j.cie.2015.12.023.
[19] Belinato G, Almeida FA de, Paiva AP de, Gomes JH de F, Balestrassi PP, Rosa PARC. A multivariate normal boundary intersection PCA-based approach to reduce dimensionality in optimization problems for LBM process. *Eng Comput* 2019;35:1533–44. https://doi.org/10.1007/s00366-018-0678-3.
[20] Almeida FA, Santos ACO, Paiva AP de, Gomes GF, Gomes JH de F. Multivariate Taguchi loss function optimization based on principal components analysis and normal boundary intersection. *Eng Comput* 2022;38:1627–43. https://doi.org/10.1007/s00366-020-01122-8.
[21] Bacci LA, Mello LG, Incerti T, Paiva AP de, Balestrassi PP. Optimization of combined time series methods to forecast the demand for coffee in Brazil: A new approach using Normal Boundary Intersection coupled with mixture designs of experiments and rotated factor scores. *Int J Prod Econ* 2019;212:186–211. https://doi.org/10.1016/j.ijpe.2019.03.001.